

Relativistic three-body bound states and the reduction from four to three dimensions*

Paul C. Dulany[†] and S. J. Wallace

*Department of Physics and Center for Theoretical Physics,
University of Maryland, College Park, Maryland 20742-4111*

(Submitted to Phys. Rev. C February 14, 1997)

(Published December 1, 1997 [Phys. Rev. C **56**, 2992])

Beginning with an effective field theory based upon meson exchange, the Bethe-Salpeter equation for the three-particle propagator (six-point function) is derived. Using the one-boson-exchange form of the kernel, this equation is then analyzed using time-ordered perturbation theory, and a three-dimensional equation for the propagator is developed. The propagator consists of a pre-factor in which the relative energies are fixed by the initial state of the particles, an intermediate part in which only global propagation of the particles occurs, and a post-factor in which relative energies are fixed by the final state of the particles. The pre- and post-factors are necessary in order to account for the transition from states where particles are off their mass shell to states described by the global propagator with all of the particle energies on shell. The pole structure of the intermediate part of the propagator is used to determine the equation for the three-body bound state: a Schrödinger-like relativistic equation with a single, global Green's function. The role of the pre- and post-factors in the relativistic dynamics is to incorporate the poles of the breakup channels in the initial and final states. The derivation of this equation by integrating over the relative times rather than via a constraint on relative momenta allows the inclusion of retardation and dynamical boost corrections without introducing unphysical singularities.

21.30.Fe, 21.45.+v, 13.75.Cs

I. INTRODUCTION

Faddeev's three-body work of 1960 [1], combined with the earlier two-body work of Bethe and Salpeter, and Gell-Mann and Low [2,3], produced significant interest within the nuclear and particle physics communities in solving the fully relativistic three-body problem [4–10]. Calculations based upon the full four-dimensional theory, however, have proved very difficult, and have only recently been performed by Rupp and Tjon using separable interactions [11].

*From a dissertation to be submitted to the Graduate School, University of Maryland, by Paul C. Dulany in partial fulfillment of the requirements for the Ph.D. degree in Physics.

[†]dulany@quark.umd.edu

In the meantime, three-dimensional nonrelativistic calculations based upon the Schrödinger equation have progressed significantly. Using NN potentials which provide a good description of two-body data, recent calculations have been performed to a precision of 10 keV [12]. Given the successes of these nonrelativistic calculations in obtaining excellent precision, discrepancies with experiment of order 10 keV or larger are due to inaccuracies in the theoretical input rather than uncertainties in the calculations. The main “missing physics” in these calculations are three-body forces and relativistic effects. A recent calculation found the triton to be underbound by roughly 480–860 keV [12]. A recent assessment of the triton potential energy suggested that a consistent relativistic calculation could account for as much as 300 keV of repulsion [13, and references therein]; however, recent relativistic calculations using the Blankenbecler-Sugar formalism and the CD-Bonn potential showed an *increased* binding of 200 keV [12]. The size of the relativistic effects determines the amount of three-body interaction that would therefore be required. A consistent relativistic three-nucleon calculation is needed in order to permit some understanding of the respective roles of relativistic effects and three-body forces in nuclear binding.

In view of the successes of the nonrelativistic calculations and the need for relativistic calculations, many three-dimensional reductions of the relativistic four-dimensional Bethe-Salpeter equation have been made following the two-body work of Blankenbecler and Sugar, and Logunov and Tavkhelidze [14–19]. This approach, often called the quasipotential approach, consists of replacing the Bethe-Salpeter equation with a set of two coupled equations. These equations involve two new functions, the quasipotential W and the quasipotential Green’s function G_{QP} . We may choose one of these functions arbitrarily. The requirement that these equations be equivalent to the Bethe-Salpeter equation then fixes the other function. Traditionally, the quasipotential Green’s function G_{QP} is chosen to contain a Dirac δ function constraint which reduces the dimensionality of one of the new equations. Difficulties with this procedure arise when the equation for the quasipotential W is truncated. What form these difficulties take is dependent upon the form of the constraint used in the quasipotential Green’s function. For example, in the Gross equation [20] this truncation introduces into the wave function unphysical singularities which must be removed by hand. In the instant formalism [21], singularities arise when attempting the dynamical boost of the wave function. Although they take different forms, the root cause of these difficulties is the δ function constraint combined with the truncation of the quasipotential. Given the difficulties with solving the full four-dimensional equation, the success of the nonrelativistic three-dimensional calculations, and the fundamental problems in the quasipotential approach, a different technique for dimensional reduction seems warranted.

In this paper we develop an approach to the relativistic three-body problem, with an emphasis on three-body bound states. We start from the Bethe-Salpeter equation for the full three-body Green’s function in momentum space. For definiteness, we use scalar meson exchange as a model for the interaction; extension to other forms of interactions is straightforward. Negative energy states are omitted as the dominant physics is obtained from positive energy states.

We perform a Fourier transformation of the zeroth component of all internal momenta to relative-time variables, and carry out the relative-time integrations, which has the effect of transforming each Feynman graph into several time-ordered graphs. These time-ordered graphs are three-dimensional in nature. Rearranging and summing graphs produces an

$$\mathcal{V}_j = \text{[diagram 1]} + \text{[diagram 2]} + \text{[diagram 3]} + \dots$$

FIG. 1. The sum of two-body-irreducible graphs denoted by \mathcal{V}_j .

expression for the full, four-dimensional, three-body Green's function in which all of the internal variables are three dimensional. It follows that the bound-state equation is three dimensional as well. We find that the propagator consists of a pre-factor in which the relative energies are fixed by the initial state of the particles, an intermediate part in which only global propagation of the particles occurs, and a post-factor in which relative energies are fixed by the final state of the particles. The pre- and post-factors are necessary in order to account for the transition from states where particles are off their mass shell to states described by the global propagator with all of the particle energies on shell. This formalism allows calculations of bound states in three-dimensions (where much success has been shown) and provides the formalism for embedding the result within a four-dimensional covariant scattering theory.

In Sec. II we define the full three-body Green's function. Then, in Sec. III we examine the three-dimensional reduction of the internal momenta of the Green's function. In Sec. IV we examine the structure of the Green's function, organizing the summation of graphs into pre- and post-factors, and a three-dimensional iterative Green's function. In Sec. V we extract the bound-state equation from the pole of the Green's function. Finally, in Sec. VI we discuss our conclusions from this work. We also provide three appendices: Appendix A, in which we provide the rules for time-ordered perturbation theory for our model, Appendix B, in which we provide more details of the reduction from four to three dimensions, and Appendix C, in which we discuss cluster separability in our formalism.

II. THE FULL THREE-BODY GREEN'S FUNCTION

The four-dimensional three-body Green's function is defined in field theory as the six-point function

$$\mathcal{G}(x_1, x_2, x_3; y_1, y_2, y_3) \equiv \langle 0 | T[\psi_1(x_1)\psi_2(x_2)\psi_3(x_3)\bar{\psi}_3(y_3)\bar{\psi}_2(y_2)\bar{\psi}_1(y_1)] | 0 \rangle . \quad (1)$$

Here we allow ψ to represent either spin-1/2 or spin-0 particles, and consider the three particles to be distinguishable. Note that with distinguishable particles, ψ_1 can only contract with $\bar{\psi}_1$, and for spin-1/2 particles anticommutes with $\bar{\psi}_2$ and $\bar{\psi}_3$. The interaction is assumed to be a sum of meson-nucleon interaction terms [see Eq. (9)].

The Bethe-Salpeter equation [2,3] for the three-body Green's function may be derived from Eq. (1) by expanding \mathcal{G} in a perturbation series in the interaction picture. Rearranging the resulting Feynman graphs into two sets, the two-body irreducible graphs and the iterative graphs, and denoting the sum of two-body irreducible graphs for cluster j as \mathcal{V}_j (see Fig. 1), we find

$$\begin{aligned} \mathcal{G} &= -ig_1g_2g_3 - \mathcal{G} \sum_{j=1}^3 \mathcal{V}_j g_k g_l = \mathcal{G}_0 + \mathcal{G} \sum_j [\mathcal{V}_j (ig_j)^{-1}] \mathcal{G}_0 \\ &= \mathcal{G}_0 + \mathcal{G}_0 \sum_j [\mathcal{V}_j (ig_j)^{-1}] \mathcal{G} , \end{aligned} \quad (2)$$

where $\mathcal{G}_0 = -ig_1g_2g_3$. (For reviews of the Bethe-Salpeter equation see Nakanishi [22] and Remiddi [23].) Note that we are considering distinguishable particles, and that the subscript of the single-particle Green's function g_j refers to the particle species. For indistinguishable particles the products would need to be symmetrized or antisymmetrized depending upon whether we are considering spin-0 or spin-1/2 particles. The index j of the interaction in Eq. (2) conforms to “odd particle out” notation, such that \mathcal{V}_j represents the sum of two-body irreducible graphs between particles k and l , where (jkl) is an even permutation of (123). The “self-energy-summed” single-particle propagator g_j is approximated by the free propagator using the physical mass,

$$g_j(x', x) \approx -i\langle 0| T[\psi_j(x')\bar{\psi}_j(x)] |0\rangle . \quad (3)$$

Although this analysis neglects Feynman diagrams representing three-body interactions, we shall see later that Eq. (2) contains *time-ordered* diagrams representing three-body interactions.

III. THREE-DIMENSIONAL REDUCTION

A three-dimensional reduction follows from decomposing graphs into sums of distinct time intervals between consecutive meson emission and absorption events, and then integrating over the duration of each interval.

In order to establish some notation, the free-particle propagator is written as the sum of a positive- and a negative-energy part

$$g(p) = \frac{N^+(\mathbf{p})}{p^0 - \epsilon(\mathbf{p}) + i\eta} - \frac{N^-(\mathbf{p})}{p^0 + \epsilon(\mathbf{p}) - i\eta} , \quad (4)$$

where the on-shell energy of a particle is denoted by

$$\epsilon_j(\mathbf{p}) \equiv \sqrt{\mathbf{p}^2 + m_j^2} , \quad (5)$$

and we define

$$N^+(\mathbf{p}) \equiv u(\mathbf{p})\bar{u}(\mathbf{p}) , \quad (6)$$

and similarly

$$N^-(\mathbf{p}) \equiv -v(-\mathbf{p})\bar{v}(-\mathbf{p}) . \quad (7)$$

For spin-1/2 particles, $u(\mathbf{p})$ is a positive-energy Dirac spinor, $v(-\mathbf{p})$ is a negative-energy Dirac spinor, $\bar{u}(\mathbf{p}) = u^\dagger(\mathbf{p})\gamma^0$, and $\bar{v}(-\mathbf{p}) = v^\dagger(-\mathbf{p})\gamma^0$. Dirac spinors obey the Hermitian normalization conditions: $u^\dagger(\mathbf{p})u(\mathbf{p}) = 1$, and $v^\dagger(-\mathbf{p})v(-\mathbf{p}) = 1$. For spin-0 particles $u(\mathbf{p}) = \bar{u}(\mathbf{p}) = 1/\sqrt{2\epsilon}$, and $v(-\mathbf{p}) = -\bar{v}(-\mathbf{p}) = 1/\sqrt{2\epsilon}$. Combining these definitions with that of Γ provided in Eq. (10), we have $\Gamma\bar{u}(\mathbf{p})u(\mathbf{p}) = g_0m/\epsilon$ and $\Gamma\bar{v}(-\mathbf{p})v(-\mathbf{p}) = -g_0m/\epsilon$ for either spin-0 or spin-1/2 particles. This notation permits the analysis to proceed on a common footing for both spins.

To facilitate the time-ordered analysis, we perform a Fourier transformation of the time-like component of the momentum of $g(p)$,

$$\begin{aligned}
g(t', t; \mathbf{p}) &\equiv \int \frac{dp^0}{(2\pi)} e^{-ip^0(t'-t)} g(p) \\
&= (-i)\theta(t' - t)N^+(\mathbf{p})e^{-i\epsilon(\mathbf{p})(t'-t)} - i\theta(t - t')N^-(\mathbf{p})e^{i\epsilon(\mathbf{p})(t'-t)}.
\end{aligned} \tag{8}$$

In order to simplify the analysis, two approximations are used:

(i) *Positive energy particles.* The contribution of negative-energy states to the propagator of Eq. (8) is neglected. This is the traditional starting point in nuclear physics. It breaks the covariance of the theory but is generally believed to be commensurate with our present understanding of nuclear forces. Extension of the analysis to incorporate negative-energy states will be left to the future.

(ii) *One boson exchange.* For NN interactions, a suitable effective interaction should describe the NN phase shifts and deuteron binding. This may be accomplished by the use of a one-boson-exchange (OBE) interaction, such that \mathcal{V}_j is replaced by the first term in Fig. 1.

Consider an interaction Hamiltonian of the form,

$$\mathcal{H}_I = \begin{cases} \sum_{j=1}^3 -g_0 : \bar{\psi}_j \varphi \psi_j :, & \text{for spin-1/2,} \\ \sum_{j=1}^3 -2m_j g_0 : \Phi_j^* \varphi \Phi_j :, & \text{for spin-0.} \end{cases} \tag{9}$$

where g_0 is a coupling constant. Separate fields are introduced for each particle in order to treat them as distinct particles.

It is convenient to define a vertex factor as follows:

$$\Gamma_j \equiv \begin{cases} g_0, & \text{for spin-1/2,} \\ 2m_j g_0, & \text{for spin-0,} \end{cases} \tag{10}$$

where the factor $2m_j$ is introduced in order that both cases have a common nonrelativistic limit. Performing a Fourier transform with respect to the timelike component of the momentum, and using the approximation in which only the one-boson-exchange potential is retained, produces

$$\mathcal{V}_j \simeq -i\Gamma_k \Gamma_l \left\{ (-i)\theta(t_k - t_l) \frac{e^{-i\omega(t_k - t_l)}}{2\omega} + (-i)\theta(t_l - t_k) \frac{e^{+i\omega(t_k - t_l)}}{2\omega} \right\}, \tag{11}$$

where $\omega = \sqrt{\mu^2 + \mathbf{q}^2}$, with μ being the meson mass and \mathbf{q} being its three momentum.

The OBE interaction together with the use of the free-particle propagator [Eq. (3)] means that the analysis pertains to the ladder approximation Feynman graphs [22].

Inserting Eqs. (8) and (11) into Eq. (2) leads to an equation for the Green's function in which all of the "internal" integrations are over the three momenta and the relative times. Each contribution can be decomposed into a sequence of time intervals between consecutive meson emission and absorption events. The integral over the time duration of each such interval may be performed analytically to produce the time-ordered perturbation theory (TOPT) rules and corresponding graphs (see Appendix A).

In order to provide a few examples, consider subgraphs that contain no initial or final particle lines, i.e., that are embedded within other graphs such that interactions separate

them from initial or final particle lines. Time intervals in which three particles propagate freely correspond to

$$\begin{array}{c} \text{---} \\ \text{---} \\ \text{---} \end{array} = \frac{1}{P^0 - \epsilon_1 - \epsilon_2 - \epsilon_3 + i\eta} \equiv G_0 \quad (12)$$

and time intervals beginning with emission of a meson and ending with its absorption correspond to

$$\begin{array}{c} \bullet \text{---} \\ \text{---} \\ \text{---} \end{array} = \frac{\Gamma_2 N_2^+}{\sqrt{2\omega_3}} \frac{1}{P^0 - \epsilon_1 - \epsilon_2 - \epsilon_3 - \omega_3 + i\eta} \frac{\Gamma_1 N_1^+}{\sqrt{2\omega_3}} \quad (13)$$

When a second meson is in flight during a time interval such as in Eq. (13), the contribution is modified to the form,

$$\begin{array}{c} \text{---} \\ \text{---} \\ \text{---} \end{array} \begin{array}{c} \bullet \text{---} \\ \text{---} \\ \text{---} \end{array} \propto \begin{array}{c} \text{---} \\ \text{---} \\ \text{---} \end{array} = \frac{\Gamma_2 N_2^+}{\sqrt{2\omega_3}} \frac{1}{P^0 - \epsilon_1 - \epsilon_2 - \epsilon_3 - \omega_1 - \omega_3 + i\eta} \frac{\Gamma_1 N_1^+}{\sqrt{2\omega_3}} \quad (14)$$

where labels of the exchanged bosons correspond to “odd-particle-out” notation. In Eq. (14), the expression on the right-hand side corresponds to the time interval and vertices within the dashed box on the left-hand side. For each distinct time interval there is a denominator equal to the total energy minus the sum of the on-shell energies of all of the particles present during that time interval. Although consideration was limited to the OBE interaction, the time-ordered rules apply quite generally and, for example, the “cross-box” diagram shown yields:

$$\begin{array}{c} \bullet \text{---} \\ \text{---} \\ \text{---} \end{array} \begin{array}{c} \bullet \text{---} \\ \text{---} \\ \text{---} \end{array} = \frac{\Gamma_1 N_{1''}^+}{\sqrt{2\omega_3'}} \frac{1}{P^0 - \epsilon_1'' - \epsilon_2 - \epsilon_3 - \omega_3' + i\eta} \\ \times \frac{\Gamma_2 N_{2''}^+}{\sqrt{2\omega_3}} \frac{1}{P^0 - \epsilon_1'' - \epsilon_2'' - \epsilon_3 - \omega_3 - \omega_3' + i\eta} \frac{\Gamma_2 N_{2'}^+}{\sqrt{2\omega_3'}} \\ \times \frac{1}{P^0 - \epsilon_1'' - \epsilon_2' - \epsilon_3 - \omega_3 + i\eta} \frac{\Gamma_1 N_{1'}^+}{\sqrt{2\omega_3}} \quad (15)$$

Note that there is an implied integration over the loop three momenta. In general there are six time-ordered diagrams corresponding to a single cross-box Feynman graph, differing by the time ordering of vertices on one particle line with respect to those on the other particle line.

The transition from four to three dimensions necessitates a reclassification of diagrams in terms of three-particle irreducibility with respect to G_0 so as to distinguish between two- versus three-body forces in the time-ordered formalism. Consider the simple, iterative Feynman (four-dimensional) diagram shown at the left of Fig. 2. The reduction from four to three dimensions produces 12 time-ordered diagrams, the sum of the first four being the

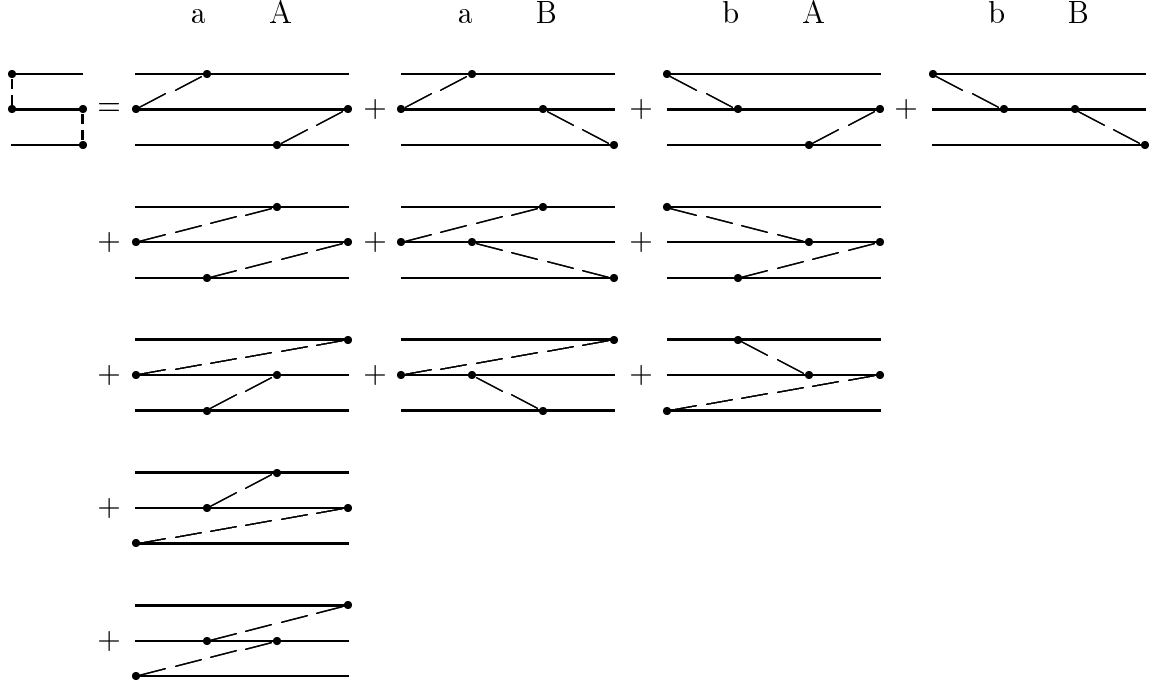


FIG. 2. By the reduction from four to three dimensions, the Feynman diagram on the left produces the 12 time-ordered diagrams on the right. Note that four of the time-ordered diagrams are iterative like the original Feynman diagram, but that the other eight are not, and constitute a three-dimensional three-body force.

iteration of the two-body force. The other eight, however, do not have the requisite time interval with only the three particles propagating, and are hence three-particle irreducible. These diagrams, along with their “sibling” diagrams (where particle two interacts with particle three before particle one), make up the three-body force V_0^{31} . The subscript denotes “zero particles out” while the superscript labels the odd-particle-out exchanges of which this graph is composed. Please see Appendix B for a fuller description of this transition from four to three dimensions.

IV. THE THREE-DIMENSIONAL THREE-BODY GREEN’S FUNCTION

Having carried out the reduction to three dimensions and reclassified the diagrams, we may re-sum the infinite series for \mathcal{G} . This sum may then be separated and factored. First, we take cluster separability into account, and then we factor the connected three-body term into three pieces.

Cluster separability [24,25] means that a Green’s function describing the propagation of clusters of particles, when there are no interactions between the clusters, consists of a product of independent factors, one for each cluster. Each cluster’s factor is the same as if the other clusters were not present. For three particles, we may have (a) no particles interacting, (b) two particles interacting and the third a spectator, and (c) all three particles interacting. As these are the only possible cases, cluster separability states that for the most general Green’s function we have

$$\begin{aligned}
\mathcal{G}(p_{1f}, p_{2f}, p_{3f}; p_{1i}, p_{2i}, p_{3i}) &= \mathcal{G}_{c;1}^{(1)}(p_{1f}; p_{1i}) \mathcal{G}_{c;2}^{(1)}(p_{2f}; p_{2i}) \mathcal{G}_{c;3}^{(1)}(p_{3f}; p_{3i}) \\
&+ \sum_{j=1}^3 \mathcal{G}_{c;j}^{(1)}(p_{jf}; p_{ji}) \mathcal{G}_{c;kl}^{(2)}(p_{kf}, p_{lf}; p_{ki}, p_{li}) \\
&+ \mathcal{G}_c^{(3)}(p_{1f}, p_{2f}, p_{3f}; p_{1i}, p_{2i}, p_{3i}) .
\end{aligned} \tag{16}$$

We are denoting a fully connected n -particle Green's function for particles j, \dots, k by $\mathcal{G}_{c;j,\dots,k}^{(n)}$. (We omit the 1, 2, 3 label for $n = 3$.) Note that the fully connected part, $\mathcal{G}_c^{(3)}$, vanishes by definition in the limit that one particle does not interact; the correct cluster limit obtains from the disconnected diagrams in this case. Note also that if a three-body bound state exists, it corresponds to a pole in $\mathcal{G}_c^{(3)}$ and has no contribution in the other parts. Please see Appendix C for a more complete discussion.

As we are primarily interested in obtaining the bound state, we discard two sets of graphs: (a) disconnected graphs in which one or more of the particles never interact, and (b) graphs in which there is an initial or final particle in every three-body-reducible time interval (i.e., in which there are no factors of G_0). (See Appendix C.) After discarding these two sets of graphs, we find that the sum of connected graphs in which there is at least one fully internal time interval is factored into three parts,

$$\mathcal{G}_c^{(3)} \longrightarrow i(2\pi)^4 \delta^{(4)}(P_f - P_i) f_{\text{post}}^{(4\text{D} \rightarrow 3\text{D})} G_3^{(3\text{D})} f_{\text{pre}}^{(3\text{D} \rightarrow 4\text{D})} . \tag{17}$$

We shall define G_3 , f_{pre} , and f_{post} shortly. The superscripts (4D \rightarrow 3D), (3D), and (3D \rightarrow 4D) label the dependence of the three parts of the Green's function on the initial-state and final-state relative energies. The superscript (3D) denotes that G_3 has no dependence upon the initial or final relative energies. As we have integrated out the internal relative energies this function is purely three dimensional. The superscript (4D \rightarrow 3D) on f_{post} denotes that it depends upon the final relative energies of the particles. This function describes the transition from the three-dimensional internal time intervals to the four dimensional final state. The function f_{pre} performs a similar function, depending upon the initial relative energies of the particles. As mentioned in Appendix C, this pattern of energy dependence is present in any fully connected Green's function that goes beyond the Born terms. However, the functional forms of the parts depend upon the number of particles involved.

We define G_3 as

$$\begin{aligned}
G_3 &\equiv G_0 \sum_{n=0}^{\infty} \left[\left(\sum_{j=1}^3 V_j N_k^+ N_l^+ + V_0 N_1^+ N_2^+ N_3^+ \right) G_0 \right]^n \\
&= G_0 + G_0 \left(\sum_{j=1}^3 V_j N_k^+ N_l^+ + V_0 N_1^+ N_2^+ N_3^+ \right) G_3 .
\end{aligned} \tag{18}$$

The three-body potential ($V_0 = V_0^{12} + V_0^{23} + V_0^{31} + V_0^{123} + \dots$) is the sum of diagrams in which (a) all three particles are interacting and (b) there are no three-particle-reducible time intervals. The three-dimensional three-body Green's function G_3 represents the sum of the diagrams in which all of the particles have interacted at least once, and will interact at least once more. This requirement ensures that interactions in G_3 are separated by the global propagator G_0 and do not contain any dependence on the initial-state and final-state particle

relative energies, i.e., are fully three dimensional. When there is a three-body bound-state pole, it is contained in G_3 .

Additional factors f_{pre} and f_{post} arise in Eq. (17) from sequences of two-body interactions of particles j and k in the initial and final states, separated by the two-body propagator for cluster l , $G_0^l \equiv 1/(P_{jk}^0 - \epsilon_j - \epsilon_k + i\eta)$, where $P_{jk}^0 = p_j^0 + p_k^0$ is the total energy of the pair. These factors may be expressed as

$$f_{\text{post}} = \frac{N_1^+ N_2^+ N_3^+}{(p_{1f}^0 - \epsilon_1 + i\eta)(p_{2f}^0 - \epsilon_2 + i\eta)(p_{3f}^0 - \epsilon_3 + i\eta)} \times \left[\sum_{j=1}^3 \sum_{k \neq j} (V_j N_k^+ N_l^+ G_0^j) \Omega_j^L \left(V_k + \frac{V_0}{2} N_k^+ \right) N_l^+ N_j^+ \right], \quad (19a)$$

$$f_{\text{pre}} = \left[\sum_{j=1}^3 \sum_{k \neq j} \left(V_k + \frac{V_0}{2} N_k^+ \right) N_l^+ N_j^+ \Omega_j^R (G_0^j V_j N_k^+ N_l^+) \right] \times \frac{1}{(p_{1i}^0 - \epsilon_1 + i\eta)(p_{2i}^0 - \epsilon_2 + i\eta)(p_{3i}^0 - \epsilon_3 + i\eta)}, \quad (19b)$$

where Ω_j^L and Ω_j^R are the left and right two-body wave operators for cluster j , defined as

$$\Omega_j^L \equiv \sum_{m=0}^{\infty} \left(V_j N_k^+ N_l^+ \frac{1}{p_k^0 + p_l^0 - \epsilon_k - \epsilon_l + i\eta} \right)^m = \sum_{m=0}^{\infty} (V_j N_k^+ N_l^+ G_0^j)^m, \quad (20a)$$

$$\Omega_j^R \equiv \sum_{m=0}^{\infty} \left(\frac{1}{p_k^0 + p_l^0 - \epsilon_k - \epsilon_l + i\eta} V_j N_k^+ N_l^+ \right)^m. \quad (20b)$$

These wave operators transform the two-body free propagator G_0^j into the full two-body Green's function G_2^j :

$$\begin{aligned} G_2^j &= G_0^j \Omega_j^L = \Omega_j^R G_0^j \\ &= G_0^j + G_0^j V_j N_k^+ N_l^+ G_2^j. \end{aligned} \quad (21)$$

Through these wave operators, the pre- and post-factors (f_{pre} and f_{post}) contain the two-body bound-state poles for the different possible clusterings of particles within the initial and final states. Note that when all particles in the initial and final states are on the mass shell, $P_{jk}^0 = P^0 - \epsilon_l$, and $G_0^l = G_0$. For consideration of interactions of the bound state with, say, a photon, one needs the full structure of \mathcal{G} , including the pre- and post-factors that allow for breakup. However, the three-body bound state is determined from consideration of G_3 as defined by Eq. (18).

V. BOUND-STATE EQUATION

Assume that there is a pole in G_3 at $P^0 = E_B(\mathbf{P})$, where $E_B(\mathbf{P}) = \sqrt{M_B^2 + \mathbf{P}^2}$, and M_B is the bound-state mass. To find the bound-state equation, we write G_3 as

$$G_3 = \frac{|\psi\rangle \langle \psi|}{P^0 - E_B + i\eta} + R, \quad (22)$$

and therefore

$$\mathcal{G}_c^{(3)} = i(2\pi)^4 \delta^{(4)}(P_f - P_i) \left[\frac{f_{\text{post}} |\psi\rangle \langle \psi| f_{\text{pre}}}{P^0 - E_B + i\eta} + f_{\text{post}} R f_{\text{pre}} \right], \quad (23)$$

where ψ is the three-dimensional TOPT analog of the Bethe-Salpeter wave function for the bound state, and R is regular at the bound-state pole. Inserting Eq. (22) into the second line of Eq. (18), taking the residue at $P^0 \rightarrow E_B$, and rearranging, we have

$$\begin{aligned} \Psi^{E_B}(\mathbf{p}_1, \mathbf{p}_2, \mathbf{p}_3) &= G_0^{E_B}(\mathbf{p}_1, \mathbf{p}_2, \mathbf{p}_3) \int \frac{d\mathbf{p}'_1}{(2\pi)^3} \frac{d\mathbf{p}'_2}{(2\pi)^3} \frac{d\mathbf{p}'_3}{(2\pi)^3} \\ &\times \left[\sum_{j=1}^3 \tilde{V}_j^{E_B}(\mathbf{p}_k, \mathbf{p}_l, \mathbf{p}_j; \mathbf{p}'_k, \mathbf{p}'_l, \mathbf{p}_j) (2\pi)^3 \delta^{(3)}(\mathbf{p}_j - \mathbf{p}'_j) \right. \\ &\quad \left. + \tilde{V}_0^{E_B}(\mathbf{p}_1, \mathbf{p}_2, \mathbf{p}_3; \mathbf{p}'_1, \mathbf{p}'_2, \mathbf{p}'_3) \right] \Psi^{E_B}(\mathbf{p}'_1, \mathbf{p}'_2, \mathbf{p}'_3), \quad (24) \end{aligned}$$

where we have defined

$$\Psi^{E_B}(\mathbf{p}_1, \mathbf{p}_2, \mathbf{p}_3) \equiv \bar{u}_1(\mathbf{p}_1) \bar{u}_2(\mathbf{p}_2) \bar{u}_3(\mathbf{p}_3) \psi^{E_B}(\mathbf{p}_1, \mathbf{p}_2, \mathbf{p}_3), \quad (25)$$

and

$$\tilde{V}_j^{E_B} \equiv \begin{cases} \bar{u}_k(\mathbf{p}_k) \bar{u}_l(\mathbf{p}_l) \left[V_j^{E_B}(\mathbf{p}_k, \mathbf{p}_l, \mathbf{p}_j; \mathbf{p}'_k, \mathbf{p}'_l, \mathbf{p}_j) \right] u_k(\mathbf{p}'_k) u_l(\mathbf{p}'_l), & \text{spin-1/2;} \\ \sqrt{\frac{m_k m_l}{\epsilon_k(\mathbf{p}_k) \epsilon_l(\mathbf{p}_l)}} \left[V_j^{E_B}(\mathbf{p}_k, \mathbf{p}_l, \mathbf{p}_j; \mathbf{p}'_k, \mathbf{p}'_l, \mathbf{p}_j) \right] \sqrt{\frac{m_k m_l}{\epsilon_k(\mathbf{p}'_k) \epsilon_l(\mathbf{p}'_l)}}, & \text{spin-0.} \end{cases} \quad (26a)$$

$$\tilde{V}_0^{E_B} \equiv \begin{cases} \bar{u}_1(\mathbf{p}_1) \bar{u}_2(\mathbf{p}_2) \bar{u}_3(\mathbf{p}_3) \left[V_0^{E_B}(\mathbf{p}_1, \mathbf{p}_2, \mathbf{p}_3; \mathbf{p}'_1, \mathbf{p}'_2, \mathbf{p}'_3) \right] u_1(\mathbf{p}'_1) u_2(\mathbf{p}'_2) u_3(\mathbf{p}'_3), & \text{spin-1/2;} \\ \sqrt{\frac{m_1 m_2 m_3}{\epsilon_1(\mathbf{p}_1) \epsilon_2(\mathbf{p}_2) \epsilon_3(\mathbf{p}_3)}} \left[V_0^{E_B}(\mathbf{p}_1, \mathbf{p}_2, \mathbf{p}_3; \mathbf{p}'_1, \mathbf{p}'_2, \mathbf{p}'_3) \right] \sqrt{\frac{m_1 m_2 m_3}{\epsilon_1(\mathbf{p}'_1) \epsilon_2(\mathbf{p}'_2) \epsilon_3(\mathbf{p}'_3)}}, & \text{spin-0.} \end{cases} \quad (26b)$$

Here the two-body interaction $\tilde{V}_j^{E_B}$, which consists of a sum of two-particle irreducible time-ordered graphs between particles k and l ($V_j^{E_B}$), multiplied by spinor factors, depends upon the momentum of the noninteracting particle \mathbf{p}_j . This is due to the term $P^0 - \epsilon_j(\mathbf{p}_j)$ in the denominator of the potential [see, for example, Eq. (13)]. As noted earlier, the connected part $\mathcal{G}_c^{(3)}$ vanishes by definition if there is a noninteracting particle. Therefore, cluster separability is unaffected by dependence of the two-body interactions that are internal to $\mathcal{G}_c^{(3)}$ on the momentum of the spectator. The bound state for a two-body cluster in the limit that the third particle does not interact (i.e., for sufficiently short-range interactions and when there are no zero-energy bound states) derives from $\mathcal{G}_c^{(2)}$ and the potentials internal to it have no dependence on the spectator momentum.

Equation (24) is a Schrödinger-like relativistic equation: it is three dimensional, has a global relativistic propagator [Eq. (12)], and reduces to the Schrödinger equation in the nonrelativistic limit. Also note that our interaction has energy dependence and hence retardation.

VI. CONCLUSION

We have examined the full three-body Green's function for the case of one-boson-exchange interactions and positive-energy spin-0 or spin-1/2 particles. We expanded out the Bethe-Salpeter equation for the Green's function into an infinite series of four-dimensional graphs. After performing a Fourier transformation of the internal energies into relative times, we integrated over the relative times, leaving an expansion of the full Green's function which only involved three-dimensional internal variables (and hence integrations), while still depending upon the full four-dimensional nature of the initial and final states.

Concentrating upon those graphs which contribute to the three-body bound-state pole, we re-summed the series into three factors: a three-dimensional Green's function G_3 obeying an iterative equation, and pre- and post-factors which link the three-dimensional G_3 to the off-shell states of the four-dimensional theory. The bound-state equation was then extracted from G_3 and shown to have a Schrödinger-like structure involving a global relativistic propagator. The one-boson-exchange potential was shown to be augmented by factors which for spin-1/2 particles are plane-wave spinors, and for spin-0 particles are kinematical factors. Although the bound state is determined without reference to them, the pre- and post-factors are needed when interactions are considered. The current must include off-shell factors to account for the introduction of four-momentum into the graph through the interaction. The complete analysis of these currents, however, is left to future papers.

Numerical calculations involving three bosons are under way. They are based upon Eq. (24) in the limit in which $\tilde{V}_0 \rightarrow 0$, and compare the full (retarded) \tilde{V}_j to an instant approximation, as well as comparing these forms to those proposed by others. Full relativistic kinematics are used in conjunction with these relativistic interactions.

ACKNOWLEDGMENTS

P.C.D. thanks the Nuclear Physics Group at the University of New Hampshire for use of their office space and their kind hospitality. Support for this work by the U.S. Department of Energy under Grant No. DE-FG02-93ER-40762 is gratefully acknowledged.

APPENDIX A: TIME-ORDERED PERTURBATION-THEORY RULES

The rules for calculating graphs in a time-ordered perturbation theory using positive-energy particles are

1. Assign an overall factor of
 - (i) $-i$ if no particles interact,
 - (ii) 1 if only two particles interact,
 - (iii) i if all three particles interact.
2. Assign a factor of $(2\pi)^4 \delta^{(4)}[\sum (p_f - p_i)]$, where the sum is over interacting particles.

3. To each particle line with no interactions between the initial and final states, assign a factor of

$$(2\pi)^4 \delta^{(4)}(p_f - p_i) N^+(\mathbf{p}_i) .$$

4. To each final particle line emerging from it's last interaction, assign a factor of

$$\frac{N^+(\mathbf{p}_f)}{p_f^0 - \epsilon + i\eta} .$$

5. For each vertex on particle j ,

- (i) Conserve 3-momentum,
- (ii) assign a factor of:

$$\frac{\Gamma_j N_j^+(\mathbf{p}'_j)}{\sqrt{2\omega(|\mathbf{p}_j - \mathbf{p}'_j|)}} ,$$

where \mathbf{p}'_j is associated with an earlier time than that with which \mathbf{p}_j is associated.

6. For each unconstrained 3-momentum \mathbf{p} , assign a factor of

$$\int \frac{d\mathbf{p}}{(2\pi)^3} .$$

7. To each time slice between vertices, assign a factor of:

$$\frac{1}{P^0 - E_1 - E_2 - E_3 - \sum_m \omega_m + i\eta} ,$$

where,

$$E_n \equiv \begin{cases} \epsilon_n = \sqrt{\mathbf{p}_n^2 + m_n^2}, & \text{for internal particles;} \\ p_n^0, & \text{for external particles,} \end{cases}$$

and m ranges over the exchanged bosons existing during the time slice.

8. For each initial line, a factor of

$$\frac{1}{p_i^0 - \epsilon + i\eta} .$$

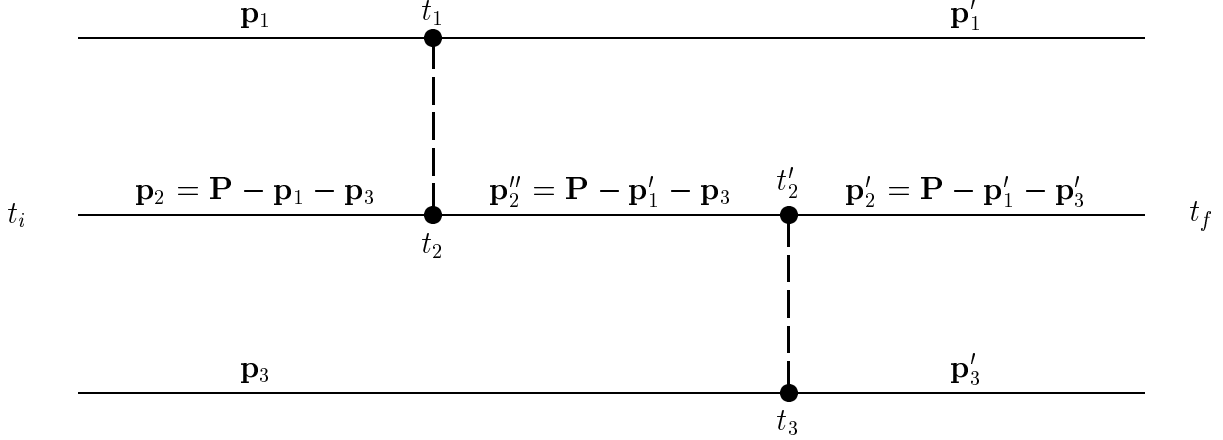


FIG. 3. An enlargement of the Feynman diagram on the left of Fig. 2. Here we also add the time and three-momentum labels used in expression (B1) to the particle lines.

APPENDIX B: REDUCTION FROM FOUR TO THREE DIMENSIONS

In Fig. 2 we have the Feynman diagram representing an interaction between particles one and two, “followed” by an interaction between particles two and three. As in Eqs. (12-14), we assume that this graph is embedded within other graphs. Using the notation of Fig. 3, our positive-energy approximation, and performing a Fourier transformation of the time-component of momentum, we have

$$\begin{aligned}
& \int dt_f \left\{ e^{iP_f^0 t_f} (-i)\theta(t_f - t_1) e^{-i\epsilon'_1(t_f - t_1)} (-i)\theta(t_f - t'_2) e^{-i\epsilon'_2(t_f - t'_2)} (-i)\theta(t_f - t_3) e^{-i\epsilon'_3(t_f - t_3)} \right\} \\
& \times \int dt_i (-1) e^{-iP_i^0 t_i} \int dt_1 dt_2 dt'_2 dt_3 \\
& \times \left(\frac{i\Gamma_2 i\Gamma_3}{2\omega_1(\mathbf{p}_3 - \mathbf{p}'_3)} \right) i \left[\overbrace{(-i)\theta(t'_2 - t_3)}^{\text{A}} e^{-i\omega_1(t'_2 - t_3)} + \overbrace{(-i)\theta(t_3 - t'_2)}^{\text{B}} e^{+i\omega_1(t'_2 - t_3)} \right] \\
& \quad \times i \left[(-i)\theta(t'_2 - t_2) N_{2n}^+ e^{-i\epsilon'_2(t'_2 - t_2)} \right] i \left[(-i)\theta(t_3 - t_i) N_3^+ e^{-i\epsilon_3(t_3 - t_i)} \right] \quad (\text{B1}) \\
& \times \left(\frac{i\Gamma_1 i\Gamma_2}{2\omega_3(\mathbf{p}_1 - \mathbf{p}'_1)} \right) i \left[\overbrace{(-i)\theta(t_1 - t_2)}^{\text{a}} e^{-i\omega_3(t_1 - t_2)} + \overbrace{(-i)\theta(t_2 - t_1)}^{\text{b}} e^{+i\omega_3(t_1 - t_2)} \right] \\
& \quad \times i \left[(-i)\theta(t_1 - t_i) N_1^+ e^{-i\epsilon_1(t_1 - t_i)} \right] i \left[(-i)\theta(t_2 - t_i) N_2^+ e^{-i\epsilon_2(t_2 - t_i)} \right]
\end{aligned}$$

where the first two lines of expression (B1) account for the fact that this graph is embedded within another graph, and we have labeled the exchanged-boson θ functions A, B, a, and b. Using the identity

$$\theta(x - y)\theta(x' - y) = \theta(x - x')\theta(x' - y) + \theta(x' - x)\theta(x - y), \quad (\text{B2})$$

one can expand the expression (B1) into the 12 terms shown in Fig. 2. The labels above the columns show from which θ functions each column originates. The top four diagrams are three-particle reducible, and are therefore representable as iterations of the two-body force. The other eight diagrams are part of the three-dimensional three-body force.

Let us choose the third diagram in the (aA) column of Fig. 2. This diagram results from the θ functions

$$\theta(t_f - t_1)\theta(t_1 - t'_2)\theta(t'_2 - t_3)\theta(t_3 - t_2)\theta(t_2 - t_i) . \quad (\text{B3})$$

Defining the time interval variables

$$\tau_5 = t_f - t_1, \quad \tau_4 = t_1 - t'_2, \quad \tau_3 = t'_2 - t_3, \quad \tau_2 = t_3 - t_2, \quad \tau_1 = t_2 - t_i, \quad \tau_0 = t_i, \quad (\text{B4})$$

and noting that $|\partial(t_f, t_1, t'_2, t_3, t_2, t_i)/\partial(\tau_5, \tau_4, \tau_3, \tau_2, \tau_1, \tau_0)| = 1$, Eq. (B1) has the form (for this particular combination of θ functions)

$$\begin{aligned} & \int d\tau_5 d\tau_4 d\tau_3 d\tau_2 d\tau_1 d\tau_0 \theta(\tau_5)\theta(\tau_4)\theta(\tau_3)\theta(\tau_2)\theta(\tau_1)\theta(\tau_0) \\ & \times (-i) e^{iP_f^0(\tau_5+\tau_4+\tau_3+\tau_2+\tau_1)} e^{i\tau_0(P_f^0-P_i^0)} e^{-i\epsilon'_1(\tau_5)} e^{-i\epsilon'_2(\tau_5+\tau_4)} e^{-i\epsilon'_3(\tau_5+\tau_4+\tau_3)} \\ & \times \left(\frac{\Gamma_2 \Gamma_3}{2\omega_1(\mathbf{p}_3 - \mathbf{p}'_3)} \right) [e^{-i\omega_1(\tau_3)}] [N_{2''}^+ e^{-i\epsilon''_2(\tau_3+\tau_2)}] [N_3^+ e^{-i\epsilon_3(\tau_2+\tau_1)}] \\ & \times \left(\frac{\Gamma_1 \Gamma_2}{2\omega_3(\mathbf{p}_1 - \mathbf{p}'_1)} \right) [e^{-i\omega_3(\tau_4+\tau_3+\tau_2)}] [N_1^+ e^{-i\epsilon_1(\tau_4+\tau_3+\tau_2+\tau_1)}] [N_2^+ e^{-i\epsilon_2(\tau_1)}] . \end{aligned} \quad (\text{B5})$$

Using the identities

$$\int_{-\infty}^{\infty} d\tau e^{i\tau(P_f^0-P_i^0)} = 2\pi \delta(P_f^0 - P_i^0) , \quad (\text{B6a})$$

$$\int_{-\infty}^{\infty} d\tau \theta(\tau) e^{i\tau(a-b+i\eta)} = \frac{i}{a-b+i\eta} , \quad (\text{B6b})$$

we can calculate the integrals in Eq. (B5). Simplifying the result, we have

$$\begin{aligned} & 2\pi \delta(P_f^0 - P_i^0) \frac{1}{P_f^0 - \epsilon'_1 - \epsilon'_2 - \epsilon'_3 + i\eta} \\ & \times \left[\frac{\Gamma_1 N_1^+}{\sqrt{2\omega_3(\mathbf{p}_1 - \mathbf{p}'_1)}} \frac{1}{P_f^0 - \epsilon_1 - \epsilon'_2 - \epsilon'_3 - \omega_3 + i\eta} \right. \\ & \times \frac{\Gamma_2 N_{2''}^+}{\sqrt{2\omega_1(\mathbf{p}_3 - \mathbf{p}'_3)}} \frac{1}{P_f^0 - \epsilon_1 - \epsilon''_2 - \epsilon'_3 - \omega_1 - \omega_3 + i\eta} \frac{\Gamma_3 N_3^+}{\sqrt{2\omega_1(\mathbf{p}_3 - \mathbf{p}'_3)}} \\ & \left. \times \frac{1}{P_f^0 - \epsilon_1 - \epsilon''_2 - \epsilon_3 - \omega_3 + i\eta} \frac{\Gamma_2 N_2^+}{\sqrt{2\omega_3(\mathbf{p}_1 - \mathbf{p}'_1)}} \right] \frac{1}{P_f^0 - \epsilon_1 - \epsilon_2 - \epsilon_3 + i\eta} . \end{aligned} \quad (\text{B7})$$

This result agrees with the rules given in Appendix. A. The effect of the pre- and post-factors on this “internal” graph is to introduce the total energy for the initial and final states. Each time interval corresponds to a denominator with the on-shell energy of each existing particle subtracted from the total energy. The graph begins and ends with a G_0 factor. Note that the graph in Fig. (2) does not include these G_0 factors. Instead it includes only those factors within the brackets. These factors are also the ones which contribute to V_0 .

APPENDIX C: CLUSTER SEPARABILITY AND TOPT

Cluster separability (CS) implies that if we describe particles propagating using a Green's function, and if one cluster of particles does not interact with another cluster of particles, then we can perform a separation of variables (between these two clusters) on the Green's function [24,25].

Let us describe three distinguishable particles propagating with initial momenta p_1, p_2, p_3 and final momenta p'_1, p'_2, p'_3 by the Green's function $\mathcal{G}(p'_1, p'_2, p'_3; p_1, p_2, p_3)$. CS tells us that in the absence of interactions, we must have

$$\mathcal{G}(p'_1, p'_2, p'_3; p_1, p_2, p_3) \longrightarrow \mathcal{G}_{c;1}^{(1)}(p'_1; p_1) \mathcal{G}_{c;2}^{(1)}(p'_2; p_2) \mathcal{G}_{c;3}^{(1)}(p'_3; p_3) . \quad (\text{C1})$$

If we have only two of the particles interacting (say 1 and 2), we have

$$\mathcal{G}(p'_1, p'_2, p'_3; p_1, p_2, p_3) \longrightarrow \mathcal{G}_{c;12}^{(2)}(p'_1, p'_2; p_1, p_2) \mathcal{G}_{c;3}^{(1)}(p'_3; p_3) . \quad (\text{C2})$$

Finally, if all three particles interact, we have the fully connected Green's function

$$\mathcal{G}(p'_1, p'_2, p'_3; p_1, p_2, p_3) \longrightarrow \mathcal{G}_c^{(3)}(p'_1, p'_2, p'_3; p_1, p_2, p_3) . \quad (\text{C3})$$

As these are the only possible cases, CS states that for the most general three-body Green's function we have Eq. (16), which we restate here

$$\begin{aligned} \mathcal{G}(p'_1, p'_2, p'_3; p_1, p_2, p_3) &= \mathcal{G}_{c;1}^{(1)}(p'_1; p_1) \mathcal{G}_{c;2}^{(1)}(p'_2; p_2) \mathcal{G}_{c;3}^{(1)}(p'_3; p_3) \\ &\quad + \sum_{i=1}^3 \mathcal{G}_{c;jk}^{(2)}(p'_j, p'_k; p_j, p_k) \mathcal{G}_{c;i}^{(1)}(p'_i; p_i) \\ &\quad + \mathcal{G}_c^{(3)}(p'_1, p'_2, p'_3; p_1, p_2, p_3) . \end{aligned} \quad (\text{16})$$

We are working in momentum space, where the Green's function is simply the result of performing a Fourier transform on the configuration space Green's function. For the n -body system,

$$\mathcal{G}(p'_1, \dots, p'_n; p_1, \dots, p_n) \equiv \int \prod_{i=1}^n d^A x_i d^A y_i e^{i(p'_i x_i - p_i y_i)} \mathcal{G}(x_1, \dots, x_n; y_1, \dots, y_n) . \quad (\text{C4})$$

Please note that some authors choose to note the Dirac δ functions explicitly, by factoring them out of the momentum space Green's functions. In this case, the left hand side of Eq. (C4) would be

$$(2\pi)^4 \delta^{(4)}(p'_1 + \dots + p'_n - p_1 - \dots - p_n) \mathcal{G}(p'_1, \dots, p'_n; p_1, \dots, p_n) \equiv \dots .$$

We have chosen not to perform this separation.

1. The TOPT case

Let us now examine the results of CS in the context of the three-body TOPT rules given in Appendix A.

a. No interactions

This case is the simplest, giving

$$\begin{aligned} \mathcal{G}(p'_1, p'_2, p'_3; p_1, p_2, p_3) &= (-i) \frac{(2\pi)^4 \delta^{(4)}(p_1 - p'_1) N^+(\mathbf{p}_1)}{p_1^0 - \epsilon_1 + i\eta} \\ &\times \frac{(2\pi)^4 \delta^{(4)}(p_2 - p'_2) N^+(\mathbf{p}_2)}{p_2^0 - \epsilon_2 + i\eta} \\ &\times \frac{(2\pi)^4 \delta^{(4)}(p_3 - p'_3) N^+(\mathbf{p}_3)}{p_3^0 - \epsilon_3 + i\eta}, \end{aligned} \quad (\text{C5})$$

which implies that

$$\mathcal{G}_{c;1}^{(1)}(p'_1; p_1) = ig_1(p'_1; p_1) = i(2\pi)^4 \delta^{(4)}(p_1 - p'_1) \frac{N^+(\mathbf{p}_1)}{p_1^0 - \epsilon_1 + i\eta}. \quad (\text{C6})$$

b. Two particles interacting

For definiteness we will assume that particles 1 and 2 are interacting, and that particle 3 is the spectator. This implies that of the four interactions V_0 , V_1 , V_2 , and V_3 , only V_3 is nonzero.

From the TOPT rules given in Appendix A, we obtain the Green's function \mathcal{G} for the case of particles 1 and 2 interacting. It is possible to write it in operator notation (defined shortly) in the form

$$\begin{aligned} \mathcal{G}(p'_1, p'_2, p'_3; p_1, p_2, p_3) &= \left\{ i(2\pi)^4 \delta^{(4)}(p_3 - p'_3) \frac{N_3^+}{p_3^0 - \epsilon_3 + i\eta} \right\} \\ &\times \left\{ (-i)(2\pi)^4 \delta^{(4)}(p_1 + p_2 - p'_1 - p'_2) \frac{N_1^+}{p_1^0 - \epsilon'_1 + i\eta} \frac{N_2^+}{p_2^0 - \epsilon'_2 + i\eta} \right. \\ &\quad \times \left([V_3^{(4D)} N_1^+ N_2^+] + [V_3^{(4D \rightarrow 3D)} N_1^+ N_2^+ (G_0^3 \Omega_3^L) V_3^{(3D \rightarrow 4D)} N_1^+ N_2^+] \right) \\ &\quad \left. \times \frac{1}{p_1^0 - \epsilon_1 + i\eta} \frac{1}{p_2^0 - \epsilon_2 + i\eta} \right\} \end{aligned} \quad (\text{C7})$$

$$= \mathcal{G}_{c;3}^{(1)}(p'_3; p_3) \mathcal{G}_{c;12}^{(2)}(p'_1, p'_2; p_1, p_2) \quad (\text{C8})$$

where the last line identifies $\mathcal{G}_{c;12}^{(2)}(p'_1, p'_2; p_1, p_2)$. First we will define the different forms of the potential V_3 , and then we will define the global propagator for cluster l , G_0^l , and the wave operator Ω_3 .

As shown in item 7 of the TOPT rules in Appendix A, the denominator of each time interval takes a different form depending upon whether all, some, or none of the particles are external (e.g. initial or final) particles. We may factor the fully connected Green's function into parts based upon the forms of these denominators and their dependence upon the initial

and final relative energies. We use the superscript (4D) to denote the part which depends upon both the initial and the final relative energies, (4D \rightarrow 3D) and (3D \rightarrow 4D) to denote transitional parts depending only upon the final or initial relative energies, respectively, and (3D) to denote the part which is independent of both the initial and final relative energies. These forms are four-dimensional, transitional, and three-dimensional, respectively. For the case of $G_c^{(2)}$, these parts are simply different forms of the two-body interaction. (The parts are more complicated for the three body case, as we see later in this Appendix and in Sec. IV.) We may see the relevant differences in these forms of the two-body interaction most easily by briefly restricting ourselves to the one-meson-in-flight approximation. Extension to the complete interaction is straightforward.

The four-dimensional form of this interaction follows from both particles being external particles. Denoting the two-body center-of-mass energy as $P_{12}^0 = p_1^0 + p_2^0$,

$$V_3^{(4D)} = \frac{\Gamma_1}{\sqrt{2\omega(|\mathbf{p}_1 - \mathbf{p}'_1|)}} \frac{1}{P_{12}^0 - p_1^0 - p_2^0 - \omega + i\eta} \frac{\Gamma_2}{\sqrt{2\omega(|\mathbf{p}_2 - \mathbf{p}'_2|)}} + \frac{\Gamma_2}{\sqrt{2\omega(|\mathbf{p}_2 - \mathbf{p}'_2|)}} \frac{1}{P_{12}^0 - p_1^0 - p_2^0 - \omega + i\eta} \frac{\Gamma_1}{\sqrt{2\omega(|\mathbf{p}_1 - \mathbf{p}'_1|)}}. \quad (C9)$$

Note that the denominator depends upon either the initial or final energies of the particles p^0 , rather than the “on-shell” energy ϵ . This is due to the fact that they are always in either initial or final states, and allows for the full four-dimensional nature of \mathcal{G} . This only appears in the Born term, in which the two particles interact only once.

The transitional form of the potential has two variants: one initial particle with one internal particle, and one final particle with one internal particle. Here we show the second variant explicitly

$$V_3^{(4D \rightarrow 3D)} = \frac{\Gamma_1}{\sqrt{2\omega(|\mathbf{q} - \mathbf{p}'_1|)}} \frac{1}{P_{12}^0 - \epsilon_1 - p_2^0 - \omega + i\eta} \frac{\Gamma_2}{\sqrt{2\omega(|\mathbf{P} - \mathbf{q} - \mathbf{p}'_2|)}} + \frac{\Gamma_2}{\sqrt{2\omega(|\mathbf{P} - \mathbf{q} - \mathbf{p}'_2|)}} \frac{1}{P_{12}^0 - p_1^0 - \epsilon_2 - \omega + i\eta} \frac{\Gamma_1}{\sqrt{2\omega(|\mathbf{q} - \mathbf{p}'_1|)}}. \quad (C10)$$

Note that each denominator depends upon one particle’s on-shell energy ϵ , and the other particle’s final energy p^0 . This is due to one particle going into its final state at the beginning of the interaction, while the other does not do so until the end of the interaction. The on-shell (internal) particle reflects our integration over the internal time variables, while the “off-shell” (final) particle reflects the (fully specified) four-dimensional nature of \mathcal{G} . The other variant of this form $V_3^{(3D \rightarrow 4D)}$ is similar, and involves the initial particle states.

Finally we have the three-dimensional form, where all of the particles are internal particles, and hence we have integrated out their energy dependence.

$$V_3^{(3D)} = \frac{\Gamma_1}{\sqrt{2\omega(|\mathbf{q} - \mathbf{q}'|)}} \frac{1}{P_{12}^0 - \epsilon_1 - \epsilon'_2 - \omega + i\eta} \frac{\Gamma_2}{\sqrt{2\omega(|\mathbf{q}' - \mathbf{q}|)}} + \frac{\Gamma_2}{\sqrt{2\omega(|\mathbf{q}' - \mathbf{q}|)}} \frac{1}{P_{12}^0 - \epsilon'_1 - \epsilon_2 - \omega + i\eta} \frac{\Gamma_1}{\sqrt{2\omega(|\mathbf{q} - \mathbf{q}'|)}}. \quad (C11)$$

Note that all of the particles are on shell, as none of them are initial or final particles. This reflects our integration over all internal time variables. This is the form which appears in the two-body bound-state equation, and is independent of the initial and final relative energies.

We have only been considering the one-meson-in-flight approximation, but these comments hold for the general case of V_3 .

We also define the two-body global propagator for cluster l

$$G_0^l \equiv \frac{1}{P_{jk}^0 - \epsilon_j - \epsilon_k + i\eta} ,$$

where $P_{jk}^0 = p_j^0 + p_k^0$ is the total energy of the pair.

It is useful to define the right and left two-body wave operators for cluster j

$$\Omega_j^L \equiv \sum_{m=0}^{\infty} \left(V_j^{(3D)} N_k^+ N_l^+ G_0^j \right)^m , \quad (\text{C12a})$$

$$\Omega_j^R \equiv \sum_{m=0}^{\infty} \left(G_0^j V_j^{(3D)} N_k^+ N_l^+ \right)^m . \quad (\text{C12b})$$

These wave operators transform the three-dimensional two-body free propagator G_0^j into the full three-dimensional two-body Green's function G_2^j :

$$\begin{aligned} G_2^j &= G_0^j \Omega_j^L = \Omega_j^R G_0^j \\ &= G_0^j + G_0^j V_j^{(3D)} N_k^+ N_l^+ G_2^j . \end{aligned} \quad (\text{C13})$$

c. All three particles interacting

Finally, we have all three particles interacting. As in the two-body case [Eq. (C7)], we may separate out the Born terms from the fully connected Greens function. In this context Born terms are defined as those in which all three-body reducible time intervals contain either an initial or final particle; there is no factor of G_0 , the three-dimensional three-body-reducible time interval. Examples of the three-body Born diagrams are given in Fig. 4. These graphs are the analog of the two-body $V_3^{(4D)}$. The simplest example is one of the terms associated with the graph in Fig. 4(d); a single TOPT three-body force. Choosing the term analogous to that shown in the second diagram in column (bA) of Fig. 2, but with external legs, we have

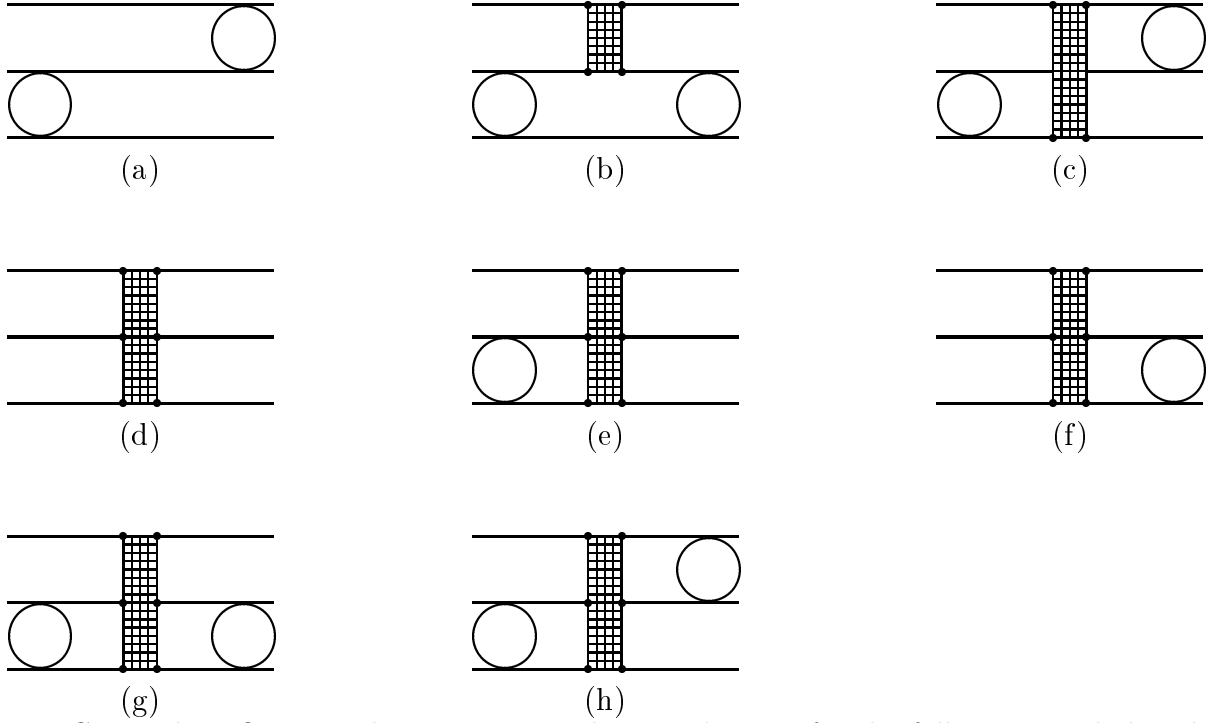


FIG. 4. The TOPT graphs representing the ‘Born’ terms for the fully-connected three-body Green’s function. The open circles represent one or more two-body forces, the boxes in graphs (b) and (c) represent two-body forces, and the boxes in graphs (d) through (h) represent three-body forces. The identifying feature is that no graphs contain a three-body reducible time interval that has no initial or final particles.

$$\begin{aligned}
V_0^{(4D)} \rightarrow & i(2\pi)^4 \delta^{(4)}(P - P') \frac{N_1^+(\mathbf{p}'_1)}{p_1^0 - \epsilon_1(\mathbf{p}'_1) + i\eta} \frac{N_2^+(\mathbf{p}'_2)}{p_2^0 - \epsilon_2(\mathbf{p}'_2) + i\eta} \frac{N_3^+(\mathbf{p}'_3)}{p_3^0 - \epsilon_3(\mathbf{p}'_3) + i\eta} \\
& \times \frac{\Gamma_2 N_2^+(\mathbf{P} - \mathbf{p}'_1 - \mathbf{p}_3)}{\sqrt{2\omega(\mathbf{p}_3 - \mathbf{p}'_3)}} \frac{1}{P^0 - p_1^0 - \epsilon_2(\mathbf{P} - \mathbf{p}'_1 - \mathbf{p}_3) - p_3^0 - \omega(\mathbf{p}_3 - \mathbf{p}'_3) + i\eta} \\
& \times \frac{\Gamma_2 N_2^+(\mathbf{p}_2)}{\sqrt{2\omega(\mathbf{p}_1 - \mathbf{p}'_1)}} \frac{1}{P^0 - p_1^0 - p_2^0 - p_3^0 - \omega(\mathbf{p}_1 - \mathbf{p}'_1) - \omega(\mathbf{p}_3 - \mathbf{p}'_3) + i\eta} \frac{\Gamma_3 N_3^+(\mathbf{p}_3)}{\sqrt{2\omega(\mathbf{p}_3 - \mathbf{p}'_3)}} \\
& \times \frac{1}{P^0 - p_1^0 - p_2^0 - p_3^0 - \omega(\mathbf{p}_1 - \mathbf{p}'_1) + i\eta} \frac{\Gamma_1 N_1^+(\mathbf{p}_1)}{\sqrt{2\omega(\mathbf{p}_1 - \mathbf{p}'_1)}} \\
& \times \frac{1}{p_1^0 - \epsilon_1(\mathbf{p}_1) + i\eta} \frac{1}{p_2^0 - \epsilon_2(\mathbf{p}_2) + i\eta} \frac{1}{p_3^0 - \epsilon_3(\mathbf{p}_3) + i\eta} . \tag{C14}
\end{aligned}$$

Note that both initial and final particle energies are needed: this is a fully four-dimensional graph.

In Sec. IV of the main text we show that when one excludes the three-body Born terms, $\mathcal{G}_c^{(3)}$ can be factored in a similar way to Eq. (C7), as shown in Eq. (17), which we repeat here for convenience

$$\mathcal{G}_c^{(3)} = i(2\pi)^4 \delta^{(4)}(P_f - P_i) f_{\text{post}}^{(4D \rightarrow 3D)} G_3^{(3D)} f_{\text{pre}}^{(3D \rightarrow 4D)} . \tag{17}$$

Here the pre- and post-factors ($f_{\text{pre}}^{(3\text{D}\rightarrow 4\text{D})}$ and $f_{\text{post}}^{(4\text{D}\rightarrow 3\text{D})}$) correspond to the transitional factors containing $V_3^{(3\text{D}\rightarrow 4\text{D})}$ and $V_3^{(4\text{D}\rightarrow 3\text{D})}$ in Eq. (C7). They connect the three-dimensional G_3 to the four dimensional external world.

It is interesting to see how $\mathcal{G}_c^{(3)}$ of Eq. (17) vanishes in the limit that one particle does not interact (i.e., for sufficiently short-range interactions and when there are no zero-energy bound states). If particle 1, say, does not interact then V_2 , V_3 , and V_0 vanish: by definition these potentials involve particle 1 interacting at least one time. This causes both f_{pre} and f_{post} [Eqs. (19)] to vanish, as they both involve factors of two of the four possible interactions (V_1 , V_2 , V_3 , and V_0), three of which must now vanish. Note that this does not require G_3 of Eq. (18) to vanish, merely the factors which multiply it in the definition of $\mathcal{G}_c^{(3)}$. In fact, even in the absence of any interactions G_3 has a nonzero value (G_0), however it is not physically meaningful; if either f_{pre} or f_{post} vanishes, then the physically meaningful $\mathcal{G}_c^{(3)}$ vanishes. Another way to state this is that $\mathcal{G}_c^{(3)}$ is fully connected, and therefore must vanish in the limit that one particle does not interact. In the factorization of $\mathcal{G}_c^{(3)}$ we have introduced, the pre- and post-factors ensure connectedness and therefore ensure that it vanishes.

- [1] L. D. Faddeev, Zh. Eksp. Theor. Fiz. **39**, 1459 (1960); [Sov. Phys. JETP **12**, 1014–1019 (1961)].
- [2] E. E. Salpeter and H. A. Bethe, Phys. Rev. **84**, 1232 (1951).
- [3] M. Gell-Mann and F. Low, Phys. Rev. **84**, 350 (1951).
- [4] J. G. Taylor, Nuovo Cimento Suppl. **1**, 857 (1963).
- [5] D. Stojanov and A. N. Tavkhelidze, Phys. Lett. **13**, 76 (1964).
- [6] V. P. Shelest and D. Stoyanov, Phys. Lett. **13**, 253 (1964).
- [7] J. G. Taylor, Phys. Rev. **150**, 1321 (1966).
- [8] M. M. Broido, Rep. Prog. Phys. **32**, 493 (1969).
- [9] D. Z. Freedman, C. Lovelace, and J. Namyslowski, Nuovo Cimento **43**, 258 (1966).
- [10] A. Tucciarone, Nuovo Cimento **41**, 204 (1966).
- [11] G. Rupp and J. A. Tjon, Phys. Rev. C **37**, 1729 (1988).
- [12] R. Machleidt, F. Summarruca, and Y. Song, Phys. Rev. C **53**, R1483 (1996), also LANL e-print nucl-th/9510023.
- [13] J. L. Friar and G. L. Payne, LANL e-print nucl-th/9601042 (unpublished).
- [14] R. Blankenbecler and R. Sugar, Phys. Rev. **142**, 1051 (1966).
- [15] A. A. Logunov and A. N. Tavkhelidze, Nuovo Cimento **29**, 380 (1963).
- [16] V. A. Alessandrini and R. L. Omnès, Phys. Rev. **139**, B167 (1965).
- [17] A. Ahmadzadeh and J. A. Tjon, Phys. Rev. **147**, 1111 (1966).
- [18] A. N. Kvinikhidze and D. T. Stoyanov, Technical Report No. E2 - 5771, Joint Institute for Nuclear Research, Dubna (unpublished).
- [19] A. Stadler and F. Gross, LANL e-print nucl-th/9607012 (unpublished).
- [20] F. Gross, J. W. Van Orden, and K. Holinde, Phys. Rev. C **45**, 2094 (1992).
- [21] N. K. Devine and S. J. Wallace, Phys. Rev. C **48**, R973 (1993).
- [22] N. Nakanishi, Suppl. Prog. Theor. Phys. **43**, 1 (1969).
- [23] E. Remiddi, in *Proceedings of the International School of Physics “Enrico Fermi”: Course*

- LXXXI*, edited by G. Costa and R. R. Gatto (North-Holland, New York, 1982), pp. 1–17.
- [24] L. L. Foldy, Phys. Rev. **122**, 275 (1961).
- [25] E. H. Wichmann and J. H. Crichton, Phys. Rev. **132**, 2788 (1963).